

# In situ probing mechanical properties of individual tungsten oxide nanowires directly grown on tungsten tips inside transmission electron microscope

K. H. Liu, W. L. Wang, Z. Xu, L. Liao, X. D. Bai, and E. G. Wang

Citation: *Appl. Phys. Lett.* **89**, 221908 (2006); doi: 10.1063/1.2397547

View online: <http://dx.doi.org/10.1063/1.2397547>

View Table of Contents: <http://aip.scitation.org/toc/apl/89/22>

Published by the [American Institute of Physics](#)

---

---



**THE WORLD'S RESOURCE FOR  
VARIABLE TEMPERATURE  
SOLID STATE CHARACTERIZATION**



OPTICAL STUDIES SYSTEMS



SEEBECK STUDIES SYSTEMS



MICROPROBE STATIONS



HALL EFFECT STUDY SYSTEMS AND MAGNETS



[WWW.MMR-TECH.COM](http://WWW.MMR-TECH.COM)

## **In situ probing mechanical properties of individual tungsten oxide nanowires directly grown on tungsten tips inside transmission electron microscope**

K. H. Liu, W. L. Wang, Z. Xu, L. Liao, X. D. Bai, and E. G. Wang<sup>a)</sup>

Beijing National Laboratory for Condensed Matter Physics, Institute of Physics, Chinese Academy of Sciences, Beijing 100080, China

(Received 22 August 2006; accepted 12 October 2006; published online 28 November 2006)

The mechanical properties of individual tungsten oxide (WO<sub>3</sub>) nanowires, directly grown onto tungsten scanning tunneling microscopy tips, have been investigated by a custom-built *in situ* transmission electron microscopy (TEM) measurement system. Young's moduli ( $E$ ) of the individual WO<sub>3</sub> nanowires were measured with the assistance of electric-induced mechanical resonance. The results indicate that  $E$  basically keeps constant at diameter larger than 30 nm, while it largely increases with decreasing diameter when diameter becomes smaller than 30 nm. This diameter dependence is attributed to the lower defect density in nanowires with smaller diameter, as imaged by *in situ* TEM. © 2006 American Institute of Physics. [DOI: 10.1063/1.2397547]

Among the various transition metal oxides, tungsten oxide (WO<sub>3</sub>) attracts the most interest in the past several decades owing to their excellent electrochromic, photochromic, and gaschromic properties, and therefore significant applications as information display, smart windows, and gas sensors.<sup>1-3</sup> Since one-dimensional WO<sub>3</sub> nanomaterials exhibit unique properties in comparison with its bulk case, many efforts have been recently made in the synthesis of the tungsten oxide nanostructures, such as nanowires,<sup>4-7</sup> nanotubes,<sup>8</sup> and nanotips.<sup>9</sup> However, the mechanical properties of the individual WO<sub>3</sub> nanowires, which play the significant role on the potential applications for nanodevice, are rarely reported. In this letter, the mechanical properties of the individual WO<sub>3</sub> nanowires will be investigated.

An *in situ* transmission electron microscopy (TEM) technique has been invented to study the mechanical properties of the individual nanomaterials.<sup>10</sup> By applying an alternating signal between the nano-object and its counter electrode, the mechanical resonance of nanomaterials is excited, and then the mechanical properties can be quantitatively determined inside TEM. Using this method, Young's moduli ( $E$ ) of nanowires,<sup>11,12</sup> nanotubes,<sup>10,13</sup> and nanobelts<sup>14</sup> have been acquired. But this technique also needs improvement. In previous reports, most of the raw nanomaterials were firstly purified with chemical solvent and then attached to the probe tip.<sup>11,13,14</sup> The purifying treatments inevitably bring contamination onto the materials, and may possibly destroy the material's structure. In addition, the method of fixing nanomaterials on the probe tip with graphite paste cannot ensure that the nanomaterials are tightly fastened, thus the measured resonance frequency of the nanomaterials often shifts out of its natural frequency. Therefore, an effective method should be developed to reliably measure the mechanical properties of the individual nano-objects.

In this letter, we report on the mechanical properties of the individual WO<sub>3</sub> nanowires directly grown onto tungsten scanning tunneling microscopy (STM) tips studied by a custom-made *in situ* TEM measurement system.<sup>15</sup> This

method can ensure that the nanowires are tightly fastened to the substrate and also avoid contamination, so the mechanical properties of WO<sub>3</sub> nanowires can be obtained reliably. The diameter dependences of Young's modulus and the mechanical quality factor were found, and the reason was revealed by the *in situ* high-resolution structural characterizations.

The tungsten STM tips were prepared by electrochemical etching and were inserted to a thermal furnace to grow WO<sub>3</sub> nanowires. The furnace was heated to 800 °C under Ar carrier gas, then CH<sub>4</sub> was introduced. The temperature was kept at 800 °C for 30 min to grow the nanowires. A similar method has been reported by other groups.<sup>4</sup> After growth, a STM tip attached with WO<sub>3</sub> nanowires was loaded into the custom-built specimen holder in a JEOL 2010 FEG TEM under the vacuum of 10<sup>-7</sup> Torr at room temperature. The STM tip was driven to approach its counterelectrode (Pt) by a piezomanipulator. A 1–10 V sine wave signal was applied across the tip and its electrode, and the resonance is stimulated by tuning the applied frequency.

It is crucial to determine the fundamental natural frequency  $\omega_0$ . Previous results show that both parametric resonance and forced resonance will either be actuated in experiments.<sup>10,16</sup> Parametric resonance occurs at  $\omega=2\omega_0/n$  ( $n$  is an integer  $\geq 1$ ),<sup>16,17</sup> and force resonance appears at  $\omega=\omega_0$  or  $\omega=\omega_0/2$ . It is important to determine the correct natural frequency  $\omega_0$ . Herein, we took a useful method to determine  $\omega_0$ . Another dc signal was adopted to adjust the vibration state; the force acting on the nanowires can be described as follows:<sup>18</sup>

$$F = \beta [Q_0 + \alpha e(V_{dc} + V_{ac} \cos 2\pi ft)]^2 = \alpha^2 \beta \{ [(W_{Pt} - W_{NW} + eV_{dc})^2 + e^2 V_{ac}^2 / 2] + 2eV_{ac}(W_{Pt} - W_{NW} + eV_{dc}) \cos 2\pi ft + e^2 V_{ac}^2 \cos 4\pi ft / 2 \}, \quad (1)$$

where  $f = \omega / 2\pi$ . Only when the nanowires vibrate under the natural frequency  $\omega_0$ , a selected dc voltage ( $eV_{dc} = W_{NW} - W_{Pt}$ ) can stop the resonance. The details can be seen elsewhere.<sup>19</sup> It is noted that the amplitude of the resonance is proportional to  $V_{ac}$ . These characteristics of fundamental

<sup>a)</sup> Author to whom correspondence should be addressed; electronic mail: egwang@aphy.iphy.ac.cn

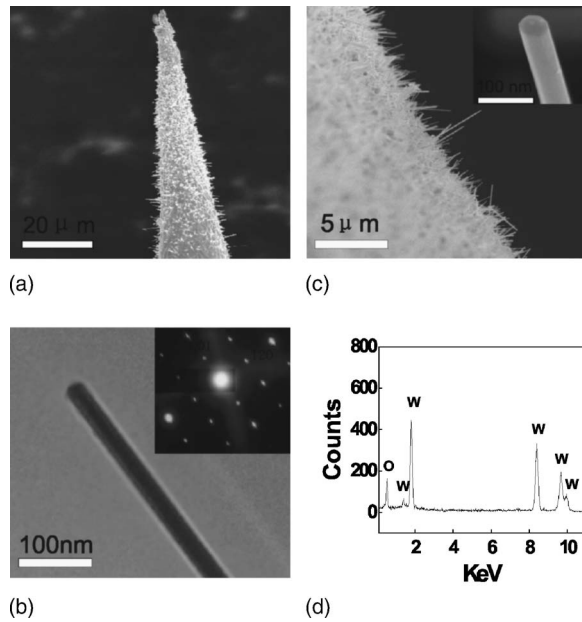


FIG. 1. (a) SEM image of the STM tip coated with  $\text{WO}_3$  nanowires. (b) Enlarged SEM image of the tip edge; the insert is the top view of one  $\text{WO}_3$  nanowire. (c) TEM image of a  $\text{WO}_3$  nanowire. The inset is its corresponding electron diffraction pattern, showing that the nanowire has monoclinic structure with the  $\langle 001 \rangle$  crystal axis oriented parallel to the long axis of the nanowires. (d) Typical EDS spectrum of the  $\text{WO}_3$  nanowires.

natural resonance can easily distinguish the  $\omega_0$  from the other resonant frequency  $\omega$ .

The length  $L$  and diameter  $D$  of nanowires were directly measured inside TEM. As mentioned before, the nanowires were directly grown onto the STM tips, they are tightly fastened at one end, the natural frequency could be accurately obtained without frequency shift, and also the high-resolution structure images of the nanowires are easily achieved by *in situ* TEM. This improved *in situ* TEM technique makes the mechanical properties of  $\text{WO}_3$  nanowires directly correspond to their high-resolution structures.

Figure 1(a) is a typical SEM image of the tungsten STM tip coated with the grown  $\text{WO}_3$  nanowires. Figure 1(b) is an enlarged image of the tip edge, showing the nanowires which usually have a length of several micrometers. The insert is the top view of one typical  $\text{WO}_3$  nanowire. Figure 1(c) shows a TEM image and its corresponding electron diffraction pattern [inset in Fig. 1(c)], indicating that the nanowires are of monoclinic structure with the  $\langle 100 \rangle$  crystal axis oriented parallel to the long axis of the nanowires. The energy dispersive spectroscopy (EDS) spectrum of the nanowires, as seen in Fig. 1(d), indicates that the products are pure  $\text{WO}_3$  nanowires.

A stationary selected  $\text{WO}_3$  nanowire is given in Fig. 2(a), which can be regarded as a vibration cantilever clamped at one end. By adjusting the frequency of the applied voltage, the natural resonance was achieved, as shown in Fig. 2(b). The root of the nanowire can be clearly imaged, so the mechanical stability can be easily displayed. Even under the large vibration amplitude for half an hour, no position shift was observed at the nanowire root and no shift of the resonance frequency was detected during this vibration. This confirms the stability of the root of the nanowires directly grown onto the STM tips.

The Euler-Bernoulli equation of a cantilevered beam was employed to analyze the mechanical properties of the  $\text{WO}_3$

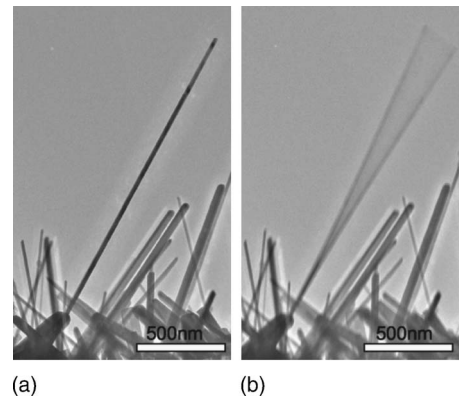


FIG. 2. Selected  $\text{WO}_3$  nanowire at (a) stationary and (b) first harmonic resonances.

nanowires. The resonance frequency ( $f_1$ ) depends on the unique intensive material parameter  $E$  (Young's modulus) and the geometric parameter of the nanowires. The nanowire was tilt at the range of  $\pm 30^\circ$ , the projection images did not show any change in diameter, illustrating that the nanowires are basically cylindrical. The amplitude at resonance was maintained below  $L/10$  to minimize the bending curvature, thus it fits the assumptions of the Euler-Bernoulli equation.<sup>20</sup> Under this condition, resonance frequency can be expressed by the following equation:

$$f_i = \frac{\beta_i^2 D}{8\pi L^2} \sqrt{\frac{E}{\rho}}, \quad (2)$$

where  $D$ ,  $L$ ,  $E$ , and  $\rho$  are the diameter, length, Young's modulus, and mass density of the nanowires, respectively.  $\beta_i$  is a constant for the  $i$ th harmonic:  $\beta_1=1.875$ ,  $\beta_2=4.694$ . Therefore, Young's modulus can be obtained from the other parameters measured by *in situ* TEM. In the meantime, the mechanical quality factor  $Q$  can also be obtained from the full width at half maximum  $\Delta f$  of the resonance peak, i.e.,  $Q=f_1/\Delta f$ . The experimental results are summarized in Table I.

Figure 3 shows the diameter dependence of Young's modulus  $E$  of the nanowires. It is indicated that  $E$  basically keeps constant at a diameter larger than 30 nm, while it largely increases with decreasing diameter when the diameter becomes smaller than 30 nm. The quality factor has the same trend: it increases with decreasing diameter.

This similar trend of size dependence of  $E$  was previously reported in other materials, such as  $\text{ZnO}$ ,<sup>12</sup>  $\text{Ag}$ , and  $\text{Pb}$  nanowires<sup>21</sup> and carbon nanotubes.<sup>10</sup> Several models are proposed to explain it. The stiffness effect of the surface<sup>12,21</sup> and the nonlinear effect of the core<sup>22</sup> were suggested to result in this size effect. In this work, if the size effect is originated

TABLE I. Measured dimensions, resonance frequency  $f$ , Young's modulus  $E$  and its error  $\delta E$ , and quality factor  $Q$  of  $\text{WO}_3$  nanowires.

$D$ (nm)	$L$ ( $\mu\text{m}$ )	$f$ (MHz)	$E$ (GPa)	$\delta E$ (GPa)	$Q$
16	1.5	6.575	313	61	...
20	1.4	6.735	159	31	610
30	1.6	6.660	118	19	...
38	3.0	2.258	105	10	590
43	1.7	8.490	119	17	...
53	3.1	3.202	123	10	520

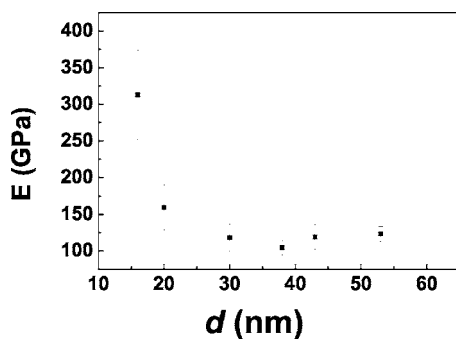


FIG. 3. Diameter dependence of Young's modulus of the  $\text{WO}_3$  nanowires.

from the stiffness effect of the surface or the nonlinear effect of the core,  $E$  will be closer to the bulk value when the diameters become larger. However, our present results show that the  $E$  of nanowires with smaller diameters is close to its bulk case. Thus the stiffness effect and the nonlinear effect can be ruled out in these results. Here, the *in situ* TEM method provides us the advantage that the microstructure can be acquired simultaneously while the mechanical properties are measured. Figure 4 shows the high-resolution TEM images of the *in situ* samples. Figures 4(a) and 4(b) are the typical lattice structures of the  $\text{WO}_3$  nanowires corresponding to the smaller and larger diameters, respectively. It is found that the large quantity of planar defects exists in the nanowires with larger diameters, which is resulted from the higher density of the oxygen vacancies in the thicker nanowires.<sup>7</sup> The difference in defect density among the

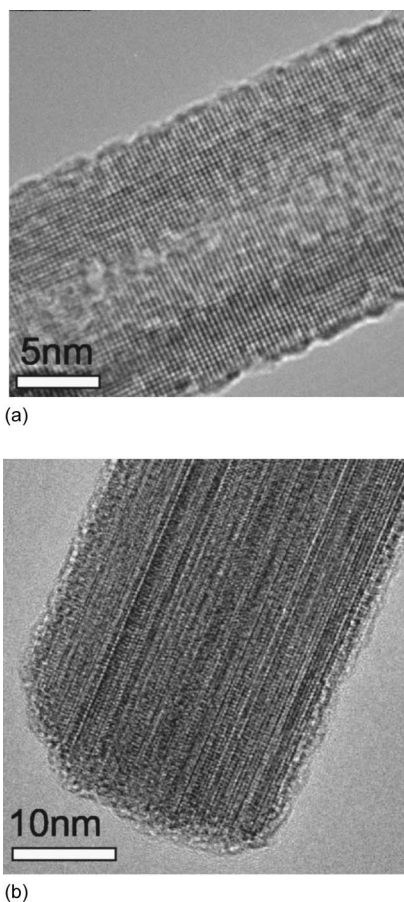


FIG. 4. Typical *in situ* high-resolution TEM images, corresponding to the nanowires with (a) smaller diameter and (b) larger diameter, respectively.

nanowires with different diameters could be the main reason for the size dependence of the mechanical properties of the  $\text{WO}_3$  nanowires. The lower defect density in the thinner nanowires [Fig. 4(a)] makes their Young's modulus close to its bulk case ( $\sim 300$  GPa).

The quality factor  $Q$  also shows a diameter dependence (Table I). The thinner  $\text{WO}_3$  nanowires have larger  $Q$  values. It is known that the inverse factor  $1/Q$  is related to the energy dissipation. Because the nanowires vibrate at TEM vacuum ( $10^{-7}$  Torr), the energy dissipation arising from air damping can be neglected; it originates mainly from the intrinsic properties of "internal friction" involving surface and defect effects. The thinner nanowires show relatively low defects, which results in less energy dissipation.

In conclusion, the mechanical properties of  $\text{WO}_3$  nanowires were investigated by *in situ* TEM method. The direct growth of nanowires onto the STM probe tip enables reliable property measurements. The mechanical properties of  $\text{WO}_3$  nanowires show a size dependence. The nanowire's Young's modulus largely increases when its diameter becomes smaller than 30 nm, which approaches its bulk value. The planar defect plays an important role on the size effect. This work also provides a reliable method to measure the other properties by directly growing nano-objects onto the probe tips.

This research was financially supported by the NSF (Grant Nos. 103024, 50472074, and 60021403), the MOST, and the CAS of China.

- <sup>1</sup>C. C. Liao, F. R. Chen, and J. J. Kai, *Sol. Energy Mater. Sol. Cells* **90**, 1147 (2006).
- <sup>2</sup>I. Turyan, U. O. Krasovec, B. Orel, T. Saraidorov, R. Reisfeld, and D. Mandler, *Adv. Mater. (Weinheim, Ger.)* **12**, 330 (2000).
- <sup>3</sup>J. L. Solis, S. Saukko, L. Kish, C. G. Granqvist, and V. Lantto, *Thin Solid Films* **391**, 255 (2001).
- <sup>4</sup>C. Klinke, J. B. Hannon, L. Gignac, K. Reuter, and P. Avouris, *J. Phys. Chem. B* **109**, 17787 (2005).
- <sup>5</sup>Z. Liu, Y. Bando, and C. Tang, *Chem. Phys. Lett.* **372**, 179 (2003).
- <sup>6</sup>G. Gu, B. Zheng, W. Q. Han, S. Roth, and J. Liu, *Nano Lett.* **2**, 849 (2002).
- <sup>7</sup>J. Zhou, L. Gong, S. Z. Deng, J. Chen, J. C. She, N. X. Xu, R. Yang, and Z. L. Wang, *Appl. Phys. Lett.* **87**, 223108 (2005).
- <sup>8</sup>Y. B. Li, Y. Bando, and D. Golberg, *Adv. Mater. (Weinheim, Ger.)* **15**, 1294 (2003).
- <sup>9</sup>J. Zhou, Y. Ding, S. Z. Deng, L. Gong, N. X. Xu, and Z. L. Wang, *Adv. Mater. (Weinheim, Ger.)* **17**, 2107 (2005).
- <sup>10</sup>P. Poncharal, Z. L. Wang, D. Ugarte, and W. A. de Heer, *Science* **283**, 1513 (1999).
- <sup>11</sup>C. Y. Nam, P. Jaroenapibal, D. Tham, D. E. Luzzi, S. Evoy, and J. E. Fischer, *Nano Lett.* **6**, 153 (2006).
- <sup>12</sup>C. Q. Chen, Y. Shi, Y. S. Zhang, J. Zhu, and Y. J. Yan, *Phys. Rev. Lett.* **96**, 075505 (2006).
- <sup>13</sup>X. D. Bai, P. X. Gao, and Z. L. Wang, *Appl. Phys. Lett.* **82**, 4806 (2003).
- <sup>14</sup>P. Jaroenapibal, D. E. Luzzi, S. Evoy, and S. Arepalli, *Appl. Phys. Lett.* **85**, 4328 (2004).
- <sup>15</sup>Z. Xu, X. D. Bai, E. G. Wang, and Z. L. Wang, *Appl. Phys. Lett.* **87**, 163106 (2005).
- <sup>16</sup>M. F. Yu, G. J. Wagner, R. S. Ruoff, and M. J. Dyer, *Phys. Rev. B* **66**, 073406 (2002).
- <sup>17</sup>K. L. Turner, S. A. Miller, P. G. Hartwell, N. C. MacDonald, S. H. Strogatz, and S. G. Adams, *Nature (London)* **396**, 149 (1998).
- <sup>18</sup>R. Gao, Z. W. Pan, and Z. L. Wang, *Appl. Phys. Lett.* **78**, 1757 (2001).
- <sup>19</sup>X. D. Bai, E. G. Wang, P. X. Gao, and Z. L. Wang, *Nano Lett.* **3**, 1147 (2003).
- <sup>20</sup>L. Meirovich, *Element of Vibration Analysis*, 2nd ed. (McGraw-Hill, New York, 1986), p. 235.
- <sup>21</sup>S. Cuenot, C. Fretigny, S. Demoustier-Champagne, and B. Nysten, *Phys. Rev. B* **69**, 165410 (2004).
- <sup>22</sup>H. Liang and M. Upmanyu, *Phys. Rev. B* **71**, 241403 (2005).